

# Refractive index sensor based on a step index multimode polymer optical fiber with a micro-hole created by a miniature numerical control machine

Gaopeng Xin (辛高鹏), Kun Peng (彭 坤), Zhimin Gu (谷志民), Jian Zhao (赵 健),  
Ruiqin Fan (范瑞琴), Lu Liu (刘 璐), and Xiaofeng Xu (徐晓峰)\*

State Key Laboratory of Superhard Materials, College of Physics, Jilin University, Changchun 130012, China

\*Corresponding author: ccxuxiaofeng@yahoo.com.cn

Received June 14, 2012; accepted September 4, 2012; posted online January 21, 2013

A compact in-fiber refractive index (RI) sensor based on a step index multimode polymer optical fiber with a micro-hole drilled by a miniature numerical control machine is presented. A good linear relationship between the transmission and RI over a large operating range from 1.335 to 1.475 and a sensitivity of 36 071.43 mV/RIU (RI unit) are found. The relationship between the transmission and the RI of the hole depends on the micro-hole's diameter and depth. The RI sensor developed in this letter is low-cost, easily fabricated, and capable of continuous measurement.

OCIS codes: 060.2370, 060.2310.

doi: 10.3788/COL201311.020601.

Refractive index (RI) silica fiber sensors, such as fiber grating-based sensors<sup>[1–3]</sup>, surface plasma resonance (SPR) RI sensors<sup>[4,5]</sup>, and Fabry-Pérot (F-P) or micro-hole fiber sensors<sup>[6–11]</sup>, among others, have attracted considerable interest in recent years. However, these sensors still feature some problems that have yet to be resolved. Grating-based silica fiber sensors are limited by their nonlinear characteristics and small RI range. Silica fiber sensors based on SPR show difficulties in coating sufficiently thin films of high quality on a fiber. Furthermore, silica fiber sensors based on F-P or micro-holes are affected by their small RI range and nonlinear response to RI variations and require expensive fabrication equipment, thus limiting their extensive application. Polymer optical fiber (POF)-based sensors are widely recognized to offer various because of their important advantages<sup>[12,13]</sup>. However, these sensors, which include biconical sensors<sup>[12]</sup>, side-polished sensor<sup>[14]</sup>, coiled shape sensors<sup>[15]</sup>, and so on, also feature several problems, such as low sensitivity, narrow operating range, and poor linear characteristics, among others<sup>[12–16]</sup>.

In this letter, we present a simple RI sensor based on a step index multimode (SIM) POF with a micro-hole drilled by a miniature numerical control machine (MNCM). The MNCM is comprised of an XYZ-axis translation stage with a numerical control unit and cutting tools of various specifications (20° V-type, speed 8000 RPM) for micro-hole machining. The fiber was mounted on the XYZ-axis translation stage with dimensions of 200×150×100 (mm), a resolution of 0.5 μm, and a repositioning accuracy of 1 μm. The structure diagram of the sensor head with a hole is shown in Fig. 1. The diameter and the depth of the hole are both 0.4 mm. To the best of our knowledge, this particular RI sensor exhibits many desirable characteristics, including easy fabrication, easy operation, excellent linearity, wide RI sensing range, low fabrication cost, potential for mass production, and so on. The sensor developed in this letter has good application prospects and can be used to

measure different types of RI.

The proposed fiber sensor system is comprised of a 650-nm semiconductor laser, a fiber sensor head, a photoelectric converter, and an oscilloscope. The sensing head is fixed to the substrate to protect the hole from shaking or bending and avoid unnecessary errors. A stable and modulated light emitted by the semiconductor laser is coupled into the fiber sensor for determining ambient variations via fiber output power detection. During the tests, the hole in the fiber is filled with a series of RI liquid samples (glycerin-water mixtures) by an injector. After the sample is measured, the hole is carefully cleaned using an ultrasonic cleaner until the transmission power is restored and no residual liquid is left inside the hole. The error attributed to temperature is negligible<sup>[17]</sup>, and the temperature is kept constant at 20 °C.

To investigate RI responses, RI measurements of the proposed sensor are carried out. In Fig. 2, the output voltage of the sensor with a hole of 0.6-mm diameter and 1-mm depth is plotted as a function of  $n_h$ , where  $n_h$  is the RI of the hole. The discrete points are the experimental results obtained from various glycerin-water mixtures. The sensor observations reveal a large range of measurements (1.335–1.475), excellent linear response to the RI of the hole, and sensitivity of 36 071.43 mV/RIU.

The characteristics of the RI response may be explained by simple ray optics. We assume that the transmission power in a fiber cross section is uniform in distribution and that the reflected light power at the hole-core

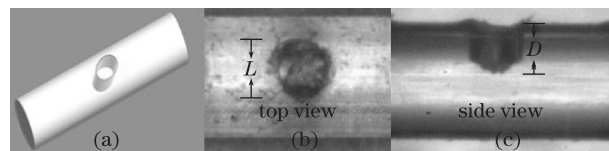


Fig. 1. (a) Geometrical drawing, (b) top view, and (c) side view of the hole. L and D represent the diameter and depth of the hole, respectively.

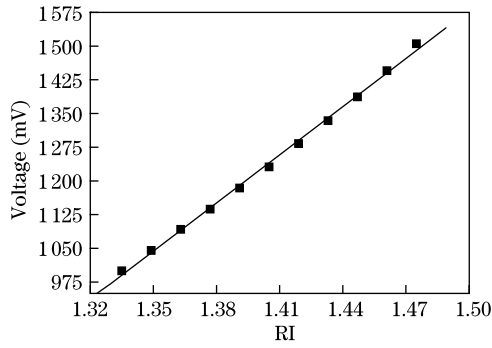


Fig. 2. Output voltage versus the RI of the hole. The dots represent the experimental data. The line represents the fitted curve.

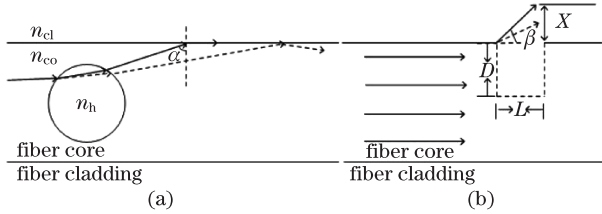


Fig. 3. (a) Relationship between the refraction of light and different RIs of the hole; (b) the divergence angle versus different RIs of the hole. The solid and dotted lines correspond to the RI of the hole from small to large.

interface may be neglected. Here, only the refraction loss caused by the hole-core interface and the orifice loss caused by the large diameter of the hole are discussed.

The transmission behavior of the light that passes through the hole is shown in Fig. 3(a), where  $n_{cl}$  (1.417) and  $n_{co}$  (1.492) represent the RIs of the fiber cladding and the fiber core, respectively, and  $n_h < n_{co}$ . Assuming that  $n_h$  is constant, the incident angle of the light (solid line) that passes through the hole is the critical angle  $\alpha$  ( $71.76^\circ$ ) at the core-cladding interface, the refraction beams of which the incident angle is smaller than the critical angle  $\alpha$  at the core-cladding interface will be dissipated through the fiber cladding. However, refraction beams that the incident angles at the core-cladding interface are larger than the critical angle  $\alpha$  will be guided. According to Snell's law, when  $n_h$  increases, the incident angle of some of the light that passes through the hole becomes larger than the critical angle at the core-cladding interface. Thus, when  $n_h$  increases, more beams are bound to the fiber core and the output voltage increases.

The orifice loss is shown in Fig. 3(b). The angle  $\beta$  represents the maximum injection angle corresponding to the optical fiber numerical aperture ( $NA = 0.467$ ) and is the largest divergence angle. This angle is determined by the core-cladding RI distribution and the RI of the receiving medium in the hole. The relations between these parameters are as

$$\sin \beta = \frac{NA}{n_h}, \quad (1)$$

$$X = L \cdot \tan \beta, \quad (2)$$

where  $X$  is the height of the leaky light projection area at the orifice of the hole. The orifice loss is determined

by the projection area and increases as the projection area increases. The projection area is related to  $X$  and becomes larger as  $X$  increases. The orifice loss depends on  $X$ . For a hole with a certain  $L$  and  $D$ , when  $n_h$  is kept constant, the beams that their divergence angles are larger than  $0^\circ$  and smaller than  $\beta$  will be dissipated through the projection area with a certain height value of  $X$ . If  $n_h$  is increased, angle  $\beta$  will decrease (as in the dotted line) according to Eq. (1). Based on Eq. (2),  $X$  will decrease, leading to a reduction in the leak beams in the orifice. This reduction will, in turn, cause more beams to be guided and the output voltage to increase.

To improve the performance of the sensor, holes of different diameters and depths are investigated in groups of experiments.

In the first set of experiments, holes with the same depth but different diameters are studied, as shown in Fig. 4(a). The output voltage of the sensors increases as the RI of the hole increases. As well, the sensitivity of the sensors gradually increases as the diameter of the hole increases. This behavior may be explained by the orifice loss. When the diameter of the hole and/or  $n_h$  changes, the value of  $X$  changes and leads to a change in the orifice loss. When  $n_h$  is kept constant,  $\beta$  also remains constant for each of the holes in this group of sensors. In contrast, the orifice loss increases as  $X$  increases because of the increase in the hole diameter. When the increment of  $n_h$  in the holes is kept constant,  $\beta$  decreases and its changes are consistent with Eq. (1). Hence, variations in  $X$  among the holes may be determined by the diameter of the hole according to Eq. (2), and the value of  $X$  greatly decreases as the diameter increases. The transmission loss also decreases with increasing speed as the diameter increases.

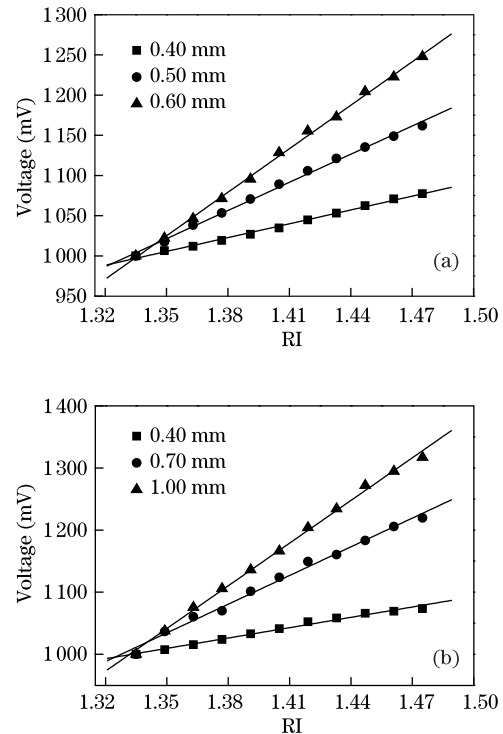


Fig. 4. (a) Output voltages versus the RIs of holes of different diameters and the same depth of 1.00 mm; (b) output voltages versus the RIs of holes of the same diameter of 0.50 mm and different depths.

In the second set of experiments, holes with the same diameter but of different depths are studied, as shown in Fig. 4(b). The output voltage of the sensors increases as the RI of the hole increases; the sensitivities of the sensors also gradually increase as the depth of the hole increases. Variations in the sensitivities of the sensors can be explained by the refraction loss. If  $n_h$  is kept constant, the refraction loss increases as the hole depth increases. However, when the increment of  $n_h$  in the hole of different depths is constant, the refraction loss greatly decreases because the greater the number of beams passing through deeper holes, the larger the number of beams that are guided because of the total reflection. Thus, the sensitivity increases as the depth of the hole increases.

In conclusion, we demonstrate a simple, compact, and low-cost RI sensor based on a SIM-POF with a micro-hole fabricated directly by a MNCM. The sensitivity of the sensor can be further improved by optimizing the hole parameters, increasing the hole number along the central axis of the fiber, changing the relations of the central axes of the holes, or using other types of POFs. The robustness of the device can be improved by limiting the hole depth and diameter in the core regions. The sensor proposed in this letter is important for biomedical, chemical, and environmental monitoring applications.

This work was supported by the National “973” Program of China (No.2011CB921603) and the National Natural Science Foundation of China (No.11074097).

## References

1. V. Bhatia and A. M. Vengsarkar, *Opt. Lett.* **21**, 692 (1996).
2. A. Kapoor and E. K. Sharma, *Appl. Opt.* **48**, G88 (2009).
3. W. Liang, Y. Huang, Y. Xu, R. K. Lee, and A. Yariv, *Appl. Phys. Lett.* **86**, 151122 (2005).
4. J. Homola, S. S. Yee, and G. Gauglitz, *Sens. Actuators B Chem.* **54**, 3 (1999).
5. D. Monzon-Hernandez and J. Villatoro, *Sens. Actuators B.* **115**, 227 (2006).
6. Z. Ran, Y. J. Rao, J. Zhang, Z. Liu, and B. Xu, *J. Lightwave Technol.* **27**, 5426 (2009).
7. Y. Wang, D. N Wang, M. W. Yang, W. Hong, and P. X. Lu, *Opt. Lett.* **34**, 3328 (2009).
8. Y. Lai, K. Zhou, L. Zhang, and I. Bennion, *Opt. Lett.* **31**, 2559 (2006).
9. Z. L. Ran, Y. J. Ra, W. J. Liu, X. Liao, and K. S. Chiang, *Opt. Express* **16**, 2252 (2008).
10. Y. Gong, T. Zhao, Y. J. Rao, Y. Wu, and Y. Guo, *Opt. Express* **18**, 15844 (2010).
11. T. Zhao, Y. Gong, Y. Rao, and Y. Wu, *Chin. Opt. Lett.* **9**, 050602 (2011).
12. H. A. Rahman, S. W. Harun, M. Yasin, S. W. Phang, S. S. A. Damanhuri, H. Arof, and H. Ahmad, *Sensor Actuator A Phy.* **171**, 219 (2011).
13. T. Yeo, T. Sun, and K. Grattan, *Sensor Actuator A Phy.* **144**, 280 (2008).
14. L. Bilro, N. J. Alberto, L. M. Sá, J. de L. Pinto, and R. Nogueira, *J. Lightwave Technol.* **6**, 864 (2011).
15. A. Armin, M. Soltanolkotabi, and P. Feizollah, *Sensor Actuator A Phy.* **165**, 181 (2011).
16. J. Arruel, F. Jiménez, G. Aldabaldetrekú, G. Durana, J. Zubia, M. Lomer, and J. Mateo, *Opt. Express* **16**, 16616 (2008).
17. T. Wei, Y. Han, Y. Li, H. L. Tai, and H. Xiao, *Opt. Express* **16**, 5764 (2008).